

Effects of the Hubble Parameter on the Cosmic Growth of the First Quasars

Rafael C. Nunes¹[★], Fabio Pacucci^{2,3}[†]

¹*Divisão de Astrofísica, Instituto Nacional de Pesquisas Espaciais, Avenida dos Astronautas 1758, São José dos Campos, 12227-010, SP, Brazil*

²*Black Hole Initiative, Harvard University, Cambridge, MA 02138, USA*

³*Center for Astrophysics | Harvard & Smithsonian, Cambridge, MA 02138, USA*

Accepted XXX. Received YYY; in original form ZZZ

ABSTRACT

Supermassive black holes (SMBHs) play a crucial role in the evolution of galaxies and are currently detected up to $z \sim 7.5$. Theories describing black hole (BH) growth are challenged by how rapidly seeds with initial mass $M_{\bullet} \lesssim 10^5 M_{\odot}$, formed at $z \sim 20 - 30$, grew to $M_{\bullet} \sim 10^9 M_{\odot}$ by $z \sim 7$. Here we study the effects of the value of the Hubble parameter, H_0 , on models describing the early growth of BHs. First, we note that the predicted mass of a quasar at $z = 6$ changes by $> 300\%$ if the underlying Hubble parameter used in the model varies from $H_0 = 65$ to $H_0 = 74 \text{ km s}^{-1} \text{ Mpc}^{-1}$, a range encompassing current estimates. Employing an MCMC approach based on priors from $z \gtrsim 6.5$ quasars and on H_0 , we study the interconnection between H_0 and the parameters describing BH growth: seed mass M_i and Eddington ratio f_{Edd} . Assuming an Eddington ratio of $f_{\text{Edd}} = 0.7$, in agreement with previous estimates, we find $H_0 = 73.6^{+1.2}_{-3.3} \text{ km s}^{-1} \text{ Mpc}^{-1}$. In a second analysis, allowing all the parameters to vary freely, we find $\log(M_i/M_{\odot}) > 4.5$ (at 95% CL), $H_0 = 74^{+1.5}_{-1.4} \text{ km s}^{-1} \text{ Mpc}^{-1}$ and $f_{\text{Edd}} = 0.77^{+0.035}_{-0.026}$ at 68% CL. Our results on the typical Eddington ratio are in agreement with previous estimates. Current values of the Hubble parameter strongly favour heavy seed formation scenarios, with $M_i \gtrsim 10^4 M_{\odot}$. In our model, with the priors on BH masses of quasars used, light seed formation scenarios are rejected at $\sim 3\sigma$.

Key words: Quasars: supermassive black holes – Cosmological parameters: H_0 – Early Universe – Dark ages, reionization, first stars

1 INTRODUCTION

Numerous surveys of the high-redshift Universe ($z \gtrsim 6$) strongly suggest that supermassive black holes (SMBHs), with masses in the range $10^6 - 10^{10} M_{\odot}$, are already in place by that cosmic age and provide the energy to power quasars (e.g., Fan et al. 2006; Wu et al. 2015; Bañados et al. 2018a). The detection of several SMBHs at redshift $z \gtrsim 7$ with masses $\sim 10^9 M_{\odot}$ is a significant challenge to the standard model of black hole (BH) growth: in fact, it is still unclear how did these BHs form and grow so rapidly over cosmic time. Current theories describe the first BH seeds to form at $z \sim 20 - 30$, less than ~ 200 Myr after the Big Bang, and then to rapidly grow, by gas accretion and mergers, to their final masses (Pacucci & Loeb 2020). Extensive reviews about the formation and early growth of quasars can be found in Gallerani et al. (2017), Latif & Schleicher (2019), and Inayoshi et al. (2019).

Over the past two decades, a large number of high- z quasars have been discovered in surveys as SDSS and the CFHQS (Jiang

et al. 2009; Willott et al. 2010), PanSTARRS1 (Bañados et al. 2016), VST/ATLAS (Carnall et al. 2015), DES (Reed et al. 2015, 2017), Subaru/HSC (Matsuoka et al. 2016), UKIDSS (Venemans et al. 2007) and VIKING (Venemans et al. 2015, 2013). Growing observational and theoretical evidence strongly suggest that the seeds at the origin of these massive objects formed at early times, likely at $z \sim 20 - 30$ (Barkana & Loeb 2001).

One possibility, the “light seeds model”, consists in these seeds being formed as remnants of the first population of stars (i.e., Population III, or Pop III, stars). While large uncertainties remain on the initial mass function of Pop III stars, several simulations and theoretical models point to a mass of the BH remnant in the range $10 \lesssim M_{\bullet}/M_{\odot} \lesssim 1000$ (e.g., Hirano et al. 2014). Alternatively, the “heavy seeds model” predicts the existence of more massive BHs, with a typical mass scale $\sim 10^5 M_{\odot}$ already at formation. These heavy seeds are named direct collapse black holes (DCBHs; e.g., Bromm & Loeb 2003; Lodato & Natarajan 2006; Pacucci et al. 2017a).

While heavy seeds could reach the $\sim 10^9 M_{\odot}$ mass scale in time to match the observations of $z \sim 7$ quasars with Eddington-limited accretion, light seeds most likely need episodes of super-

[★] E-mail: rafadcnunes@gmail.com

[†] BHI & Clay Fellow

Eddington accretion (Haiman & Loeb 2001; Volonteri & Rees 2005; Pelupessy et al. 2007; Tanaka & Haiman 2009a; Madau et al. 2014; Volonteri et al. 2015; Pacucci et al. 2015; Begelman & Volonteri 2017; Regan et al. 2019).

In addition to these two baseline formation channels, additional scenarios have been proposed, such as BHs formed from stellar collisions (Devecchi & Volonteri 2009; Devecchi et al. 2012; Katz et al. 2015) and black hole mergers (Davies et al. 2011; Lupi et al. 2014).

Currently, six quasars are known at $z > 7$ (Inayoshi et al. 2019). The farthest one thus far is J1342+0928 at $z = 7.54$ with $\sim 7.8 \times 10^8 M_\odot$ (Bañados et al. 2018a). Future surveys in the electromagnetic spectrum like Lynx (The Lynx Team 2018), AXIS (Mushotzky et al. 2019), Athena (Barret et al. 2020) and the James Webb Space Telescope, as well as surveys in the gravitational wave realm, e.g. LISA (Amaro-Seoane et al. 2017), will provide invaluable information about the formation and the growth process of high- z BH seeds (Pacucci & Loeb 2020).

Remarkably, any prediction on how BHs grow over cosmic time depends on the underlying cosmology assumed. A modification in the value of the cosmological parameters used, and/or any extension beyond the concordance Λ CDM cosmology, could significantly change the evolution and the dynamics of the Universe, possibly producing very different predictions for BH growth. Particular attention should be granted to estimates of the Hubble parameter, H_0 , which describes the current expansion rate of the universe. The most recent analyses of the Cosmic Microwave Background (CMB) observations by the Planck collaboration, assuming the Λ CDM scenario, obtained $H_0 = 67.4 \pm 0.5 \text{ km s}^{-1} \text{ Mpc}^{-1}$ (Planck Collaboration et al. 2018). A model-independent local measurement by the Hubble Space Telescope (HST) suggested instead $H_0 = 74.03 \pm 1.42 \text{ km s}^{-1} \text{ Mpc}^{-1}$ (Riess et al. 2019), which is in 4.4σ tension with Planck's estimate. Additionally, the H0LiCOW collaboration reports $H_0 = 73.3^{+1.7}_{-1.8} \text{ km s}^{-1} \text{ Mpc}^{-1}$ (Wong et al. 2019). Another accurate independent measure was carried out in Freedman et al. (2019), showing that $H_0 = 69.8 \pm 0.8 \text{ km s}^{-1} \text{ Mpc}^{-1}$. These are the most robust estimates of H_0 available in literature. As noted, there is a high degree of statistical divergence between them. This observed tension could be a signal of additional fundamental new physics beyond the standard Λ CDM model (see, e.g., Verde et al. 2019; Kumar et al. 2019 and references therein).

Here, we aim to understand the effect of the value of H_0 on models for early BH growth. First, we show how the predicted mass at $z = 6$ can be significantly affected by the choice of H_0 . Then, we constrain H_0 using information from the mass of the farthest quasars detected thus far, in the range $6.5 < z < 7.54$, assuming that mass growth occurs mostly by gas accretion. Conversely, we then study how much H_0 , assumed a free parameter, can influence our estimate of the parameters that quantify the BH growth.

This study is organized as follows. In Sec. 2 we revise the theoretical model used to describe the evolution of BH mass over cosmic time. In Sec. 3 we present our data sets and in Sec. 4 our main results and discussions. Finally, Sec. 5 summarizes our conclusions and presents some future perspectives.

2 THE COSMIC GROWTH OF BLACK HOLES

In this section we review the theoretical framework used to describe the cosmic growth of BHs via gas accretion, from seed formation ($z \sim 20 - 30$) to the observation of the farthest quasars ($z \gtrsim 6.5$). The formalism adopted here is described extensively in Pacucci

et al. (2015) and Pacucci et al. (2017b) (see also, e.g., Shapiro 2005; Ricarte & Natarajan 2018).

The evolution in cosmic time t of the BH mass M_\bullet , starting from an initial mass of the seed M_i , is usually described with the following set of three parameters:

- (i) The matter-to-energy conversion efficiency factor ϵ , which describes the fraction of rest-mass energy that is radiated away during gas accretion. The efficiency factor ϵ is defined as:

$$\epsilon = \frac{L}{\dot{M}c^2}, \quad (1)$$

where \dot{M} is the accretion rate onto the BH and L is its luminosity. The factor ϵ is customarily assumed to be $\sim 10\%$ for radiatively efficient accretion disks (Shakura & Sunyaev 1976). In case of optically thick accretion disks, or radiatively inefficient accretion flows (or RIAF), the factor ϵ can be significantly lower (see, e.g., Narayan & McClintock 2013).

- (ii) The Eddington ratio, which parametrizes the accretion rate \dot{M} on a BH of mass M_\bullet in terms of the Eddington accretion rate $\dot{M}_{\text{Edd}} \approx 2.2 \times 10^{-8} (M_\bullet / M_\odot) M_\odot \text{ yr}^{-1}$:

$$f_{\text{Edd}} = \frac{\dot{M}}{\dot{M}_{\text{Edd}}}. \quad (2)$$

- (iii) The duty cycle \mathcal{D} , quantifying the fraction of time spent accreting (i.e., the continuity of mass inflow). It is worth noting that typical quasar timescales are of order $\sim 100 \text{ Myr}$.

If we assume that the accretion rate is dominated by baryonic matter, then the BH growth rate is found with the following expression (see, e.g., Shapiro 2005; Pacucci et al. 2017b):

$$\dot{M} = \frac{\mathcal{D} f_{\text{Edd}} (1 - \epsilon) M}{\epsilon \tau}, \quad (3)$$

where τ is the characteristic accretion timescale, or Salpeter timescale (Salpeter 1955), $\tau \approx 0.45 \text{ Gyr}$.

In general, the matter-to-energy conversion efficiency factor ϵ is a strong function of the BH spin (e.g., Bardeen 1970; Novikov & Thorne 1973; Narayan & McClintock 2013). The efficiency for disk accretion onto a Schwarzschild (i.e., non-rotating) BH is $\epsilon = 0.057$, while for a Kerr, maximally rotating BH the value is found to be $\epsilon \sim 0.32$. In fact, for rotating BHs the accretion disk extends farther inwards, closer to the event horizon, so that a larger fraction of its energy can be radiated away. As we do not track the spin evolution in our work, in what follows we assume $\epsilon = 0.1$.

If we assume that ϵ , \mathcal{D} and f_{Edd} are constant between t_i and t , we can easily integrate Eq. (3), obtaining:

$$M(t) = M(t_i) \exp \left[\frac{\mathcal{D} f_{\text{Edd}} (1 - \epsilon)}{\epsilon} \frac{t - t_i}{\tau} \right], \quad (4)$$

where t_i is the initial time when the BH has a mass M_i . The lookback time as a function of z can be written as

$$t_i(z_0) = t(z_0) - t(z_i) = \frac{1}{H_0} \int_{z_0}^{z_i} \frac{dz'}{(1+z')E(z')}, \quad (5)$$

where $E(z) = H(z)/H_0$ is the ratio between the Hubble parameter at z and its current value. The value $t_i(z_0)$ is the age of the object at redshift z_0 , assuming that it formed at redshift z_i . For our purposes, z_0 is the redshift where the quasar is detected, and z_i is the redshift at seed formation.

Assuming that BH growth occurred only via baryonic gas accretion is certainly an approximation. A more realistic scenario

Table 1. Summary information of the compilation of quasars at high z adopted in this work.

Name	$M(M_\odot)$	z
J1342+0928	$(7.8^{+3.3}_{-1.9}) \times 10^8$	7.54
J1243+0100	$(3.3 \pm 2) \times 10^8$	7.07
J1120+0641	$(2.0^{+1.5}_{-0.7}) \times 10^9$	7.085
J0038-1527	$(1.33 \pm 0.25) \times 10^9$	7.021
J2348-3054	$(2.1 \pm 0.5) \times 10^9$	6.90
J0109-3047	$(1.5 \pm 0.4) \times 10^9$	6.80
J0305-3150	$(9.5^{+0.8}_{-0.7}) \times 10^8$	6.61
P036+03	$(1.9^{+1.1}_{-0.8}) \times 10^9$	6.54

would allow for additional growth channels, e.g. black hole mergers and contributions from dark matter (collisionless and self-interacting species). Recent studies (e.g., Pacucci & Loeb 2020) have shown that gas accretion is significantly dominant over mergers for the growth of BHs with $M_\bullet \gtrsim 10^5 M_\odot$ in the early Universe ($z \gtrsim 6$). For this reason, we believe that our model including only gas accretion is, to the first order, a good approximation of how BHs grew at early cosmic epochs.

3 METHODOLOGY AND DATA SET

In the following we briefly describe the data sets we use to explore the parameter space of our model.

Mass estimates for $z \geq 6.5$ quasars: We consider quasars in the redshift range $z \in [6.5, 7.54]$, i.e. up to the farthest quasar detected thus far. In particular, we consider the following sources: J2348-3054 ($z = 6.9018$, Venemans et al. 2016), J0109-3047 ($z = 6.7909$, Venemans et al. 2016), J0305-3150 ($z = 6.6145$, Venemans et al. 2016), P036+03 ($z = 6.5412$, Venemans et al. 2015; Bañados et al. 2015), J1342+0928 ($z = 7.541$, Bañados et al. 2018b), J1243+0100 ($z = 7.07$, Matsuoka et al. 2019), J1120+0641 ($z = 7.085$, Mortlock et al. 2011) and J0038-1527 ($z = 7.021$, Wang et al. 2018). This information is summarized in Table 1. Hence, we include in our analysis all $z > 7$ quasars from Inayoshi et al. (2019) for which an error bar for the mass is reported, and some quasars in the range $z \in [6.5, 7.0]$ for which the error bars are small, i.e. the mass is known typically within a factor ~ 2 . There are currently ~ 16 confirmed quasars within $z \in [6.5, 7.0]$ (see the NASA/IPAC Extragalactic Database, NED, and, e.g., Matsuoka et al. 2016) but some of these sources are characterized by very large uncertainties for the BH mass, or it is unconstrained altogether. In order to maximize the accuracy of our Markov Chain Monte Carlo method, we choose to limit the sources in our sample.

Measurement of the Hubble parameter: We adopt the latest measurements of the Hubble parameter obtained in a model-independent way. In particular, we use:

- (i) The re-analysis of the HST data using Cepheids as calibrators (Riess et al. 2019), which led to a value $H_0 = 74.03 \pm 1.42 \text{ km s}^{-1} \text{ Mpc}^{-1}$. We refer to this data point as R19.
- (ii) The recent determination of H_0 from the Tip-of-the-Red-Giant-Branch approach (Freedman et al. 2019), which led to a value $69.6 \pm 2.0 \text{ km s}^{-1} \text{ Mpc}^{-1}$, including systematic. We refer to this data point as F20.

BH growth model: In our analysis we assume a flat- Λ CDM

model as background scenario. Thus, our BH growth model is completely described by the following parameters: the seed initial mass M_i , the redshift formation of the BH z_i , the Hubble parameter H_0 , the matter density parameter (baryons + dark matter) Ω_m , the Eddington ratio f_{Edd} and the duty cycle \mathcal{D} . To decrease the complexity of this 6-dimensional parameter space, we make the following, physically motivated assumptions: (i) we fix $\Omega_m = 0.31$, (ii) we fix $z_i = 25$, and (iii) we fix $\mathcal{D} = 1$. The first assumption is motivated by the fact that the concordance flat- Λ CDM model seems to be characterized by smaller uncertainties on Ω_m than on H_0 (Planck Collaboration et al. 2018). The second assumption is supported by several models in early structure formation indicating that the formation of the first BHs occurred in the redshift range $20 \lesssim z \lesssim 30$ (e.g., Barkana & Loeb 2001; Inayoshi et al. 2019). As there is only a difference $\lesssim 100 \text{ Myr}$ in cosmic time within this redshift range, comparable to the typical quasar lifetime, we choose to fix $z_i = 25$ as the mid-point of this range of interest. This is further supported by our preliminary analysis, during which we noticed that any value within the flat prior $z_i \in [20, 30]$ does not change our main results. The third assumption stems from the fact that the Eddington ratio f_{Edd} and the duty cycle \mathcal{D} are completely degenerate in any BH growth model. Hence, we assume $\mathcal{D} = 1$ and interpret the Eddington ratio as averaged over sufficiently long timescales, typically of the order of the quasar lifetime, i.e. $\sim 100 \text{ Myr}$. This assumption is based on semi-analytical models (e.g., Tanaka & Haiman 2009b) as well as measurements of clustering of quasars at $z \gtrsim 6$ (Shen et al. 2007; Shankar et al. 2009).

We use the Markov Chain Monte Carlo (MCMC) method to analyze the parameters $\theta_i = \{M_i, H_0, f_{\text{Edd}}\}$, building the posterior probability distribution function

$$p(D|\theta) \propto \exp\left(-\frac{1}{2}\chi^2\right), \quad (6)$$

where

$$\chi^2 = \sum_i^N \left(\frac{M - M_{\text{th}}}{\sigma_M} \right)^2 + \left(\frac{H_0 - H_{0,\text{th}}}{\sigma_{H_0}} \right)^2. \quad (7)$$

Here, N runs over all quasars in Table 1, M_{th} , M and σ_M are the theoretical BH growth rate defined in Eq. (4), the observational measurement and associated error on the mass of the quasars reported in Table 1, respectively. The quantities H_0 and $H_{0,\text{th}}$ represent the model-independent measurement of the Hubble parameter and its theoretical expectation inferred from the BH growth, respectively.

The goal of any MCMC approach is to draw N samples θ_i from the general posterior probability density

$$p(\theta_i, \alpha|D) = \frac{1}{Z} p(\theta, \alpha) p(D|\theta, \alpha), \quad (8)$$

where $p(\theta, \alpha)$ and $p(D|\theta, \alpha)$ are the prior distribution and the likelihood function, respectively. Here, the quantities D and α are the set of observations and possible nuisance parameters. The amount Z is a normalization term.

We subdivided our analysis in three steps: (i) we analyze the SMBH data only, assuming fixed values for the Eddington ratio f_{Edd} ; (ii) we analyze the SMBH data only with all parameters free; (iii) we consider the joint analysis SMBH + R19 and SMBH + F20 data.

We perform the statistical analysis based on the *emcee* algorithm (Foreman-Mackey et al. 2013), assuming the theoretical model described in Sec. 2 and the following priors on the parameters baseline: $H_0 \in [10, 90]$, $M_i \in [10^2, 10^5]$, and $f_{\text{Edd}} \in [0.1, 1.5]$

in our overall analysis. We discard the first 20% steps of the chain as burn-in. We follow the Gelman-Rubin convergence criterion (Gelman & Rubin 1992), checking that all parameters in our chains have $R - 1 < 0.01$, where the parameter R quantifies the Gelman-Rubin statistic, also known as the potential scale reduction factor. It is recommended that $R < 1.1$ for all model parameters, in order to be confident that convergence is reached. We note $R < 1.01$ in our chains. We carry out a marginalization on $\Omega_m = 0.31$.

A flat prior on the seed mass $M_i \in [10^2, 10^5]$ allows both light and massive seeds (see our Sec. 1) to be included in the analysis. A flat prior on the Eddington ratio $f_{\text{Edd}} \in [0.1, 1.5]$ allows us to consider both sub-Eddington accretion rates and super-Eddington accretion rates, up to 50% above Eddington. Super-Eddington accretion rates are predicted to be common at high- z , due to a large availability of cold gas. Simple estimates presented in Begelman & Volonteri (2017) suggest that a fraction $\sim 10^{-3}$ of active galactic nuclei could be accreting at super-Eddington rates already at $z \sim 1$.

4 RESULTS AND DISCUSSION

In the following we explore the parameter space $(M_i, H_0, f_{\text{Edd}})$ with our MCMC approach, in order to constrain the probability distribution of the main parameters characterizing the growth of early BHs.

As a case study, in Fig. 1 we show an example of BH mass growth as a function of z for four values of H_0 . For simplicity, we assume $f_{\text{Edd}} = 1$, $\mathcal{D} = 1$ and initial seed mass of $M_i = 100 M_\odot$ at $z_i = 25$. In Fig. 2 we show the percentage difference between $M_\bullet^{\text{Planck}}$ and $M_\bullet^{H_0}$ (i.e., the mass computed assuming the Planck's value of H_0 or a generic value) as a function of redshift in the range $z \in [6, 10]$, in order to quantify how different H_0 values can influence the cosmic evolution of M_\bullet . The differences in the BH mass evolution for $z \gtrsim 15$ are minimal, as the cosmic time from the seeding redshift $z_i \sim 25$ is very short, i.e. $\Delta t \sim 100$ Myr. On the contrary, we note that for $z \lesssim 15$ the differences in the predicted BH mass start to become significant. In particular, assuming different H_0 values and keeping Ω_m constant, we note significant changes in the final mass at a given z value. Specifically, Fig. 2 shows that at $z = 6$ the BH mass computed assuming $H_0 = 65 \text{ km s}^{-1} \text{Mpc}^{-1}$ and $H_0 = 74 \text{ km s}^{-1} \text{Mpc}^{-1}$ differs by $\sim 48\%$ and $\sim 300\%$, respectively, from the mass computed assuming the fiducial Planck's value. As all SMBHs observed thus far are at $z < 10$ and given the current tension in the measurement of H_0 , analyzing how the value of this parameter can affect the BH mass evolution and, conversely, how observations of quasars can constrain the cosmological parameters is certainly very relevant.

As a first step in our statistical analysis, we only vary the seed mass M_i and H_0 , fixing the Eddington ratio at some physically motivated value, specifically at $f_{\text{Edd}} = 0.7$. This sustained rate is supported by the fact that at $z \gtrsim 6$ most of the BHs are predicted to be accreting close to, or even above, the Eddington rate (Begelman & Volonteri 2017), due to a large availability of cold gas. Because of our assumption of $\mathcal{D} = 1$, we keep the value of f_{Edd} below unity. In Fig. 3 we show the parametric space in the plane $\log(M_i/M_\odot) - h$, where h is the reduced Hubble parameter. We find $\log(M_i/M_\odot) > 4.5$ at 95% confidence level (CL). This result clearly indicates a preference for heavy seeds over light seeds to match the observation of the earliest quasars. For the Hubble parameter, we find $H_0 = 73.6^{+1.2}_{-3.3} \text{ km s}^{-1} \text{Mpc}^{-1}$ at 68% CL, in substantial agreement with the measurement by Riess et al. (2019). Considering the 95% CL bounds, instead, we note that H_0 may extend to lower

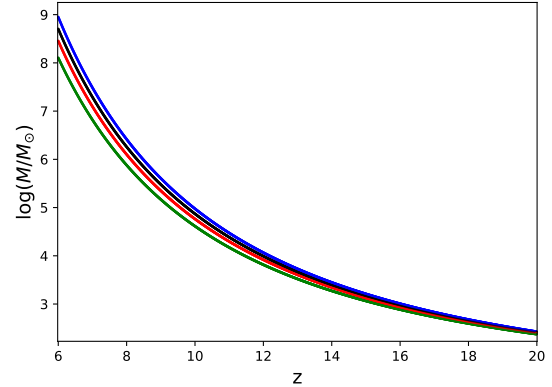


Figure 1. BH mass evolution as a function of redshift, assuming different values of the Hubble parameter: $H_0 = 65 \text{ km s}^{-1} \text{Mpc}^{-1}$, $H_0 = 67.4 \text{ km s}^{-1} \text{Mpc}^{-1}$ (Planck best fit value), $H_0 = 70 \text{ km s}^{-1} \text{Mpc}^{-1}$ and $H_0 = 74 \text{ km s}^{-1} \text{Mpc}^{-1}$ in blue, black, red and green, respectively. We assume as input values $M_i = 100 M_\odot$ at $z_i = 25$, $\Omega_m = 0.31$, $f_{\text{Edd}} = 1$ and $\mathcal{D} = 1$.

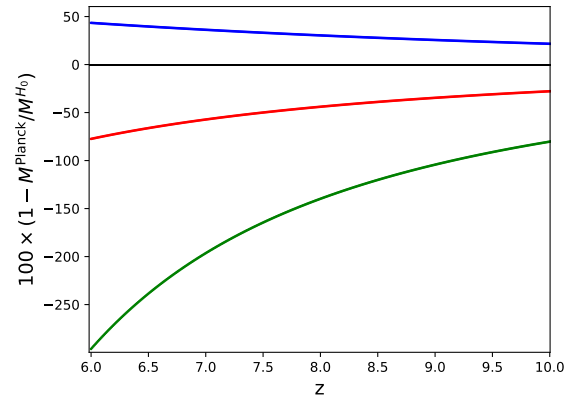


Figure 2. Percentage difference between $M_\bullet^{\text{Planck}}$ and $M_\bullet^{H_0}$ as a function of redshift in the range $z \in [6, 10]$. $M_\bullet^{\text{Planck}}$ represents the value of mass computed assuming the best-fit estimate of H_0 from Planck and $M_\bullet^{H_0}$ the mass computed assuming $H_0 = 65, 70, 74 \text{ km s}^{-1} \text{Mpc}^{-1}$, in blue, red and green, respectively. The black, thin line represents $M_\bullet^{\text{Planck}}$.

values, which are compatible with high- z measurements from the CMB. As mentioned in Sec. 1, there is a significant tension on H_0 when comparing very high- z measures from CMB data with local measures.

As a second step, we vary the parameters of the entire space M_i, H_0 and f_{Edd} , while fitting the data for our sample of $z \gtrsim 6.5$ SMBHs. The results are shown in the left panel of Fig. 4. In this global analysis, our results are as follows: $\log(M_i/M_\odot) > 4.26$, $H_0 > 55 \text{ km s}^{-1} \text{Mpc}^{-1}$ and $f_{\text{Edd}} = 0.995^{+0.076}_{-0.456}$. The lower bound on the initial mass is at 95% CL, while the other constraints are at 68% CL. If we leave all three parameters of our BH growth model free, we notice that the constraints on H_0 are loose, certainly not competitive when compared to other robust cosmological tests. In principle, fixing certain parameters in the BH growth model can lead to robust constraints on H_0 , when fitting to data from the farthest quasars. Unfortunately, constraining growth parameters is

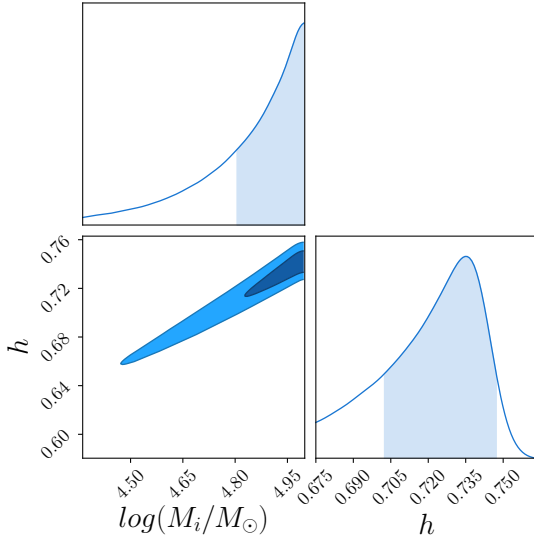


Figure 3. Two-dimensional, marginalized distributions in the parametric space $\log(M_i/M_\odot) - h$ at 1σ and 2σ CL from our SMBHs compilation data. We fix $f_{\text{Edd}} = 0.7$ and indicate with h the reduced Hubble parameter, $H_0/100$, in units of $\text{km s}^{-1}\text{Mpc}^{-1}$.

far from straightforward, as they can significantly vary from one BH to another.

In order to improve the estimates in our baseline parameters, we analyze the data combination SMBH + R19 and SMBH + F20. It is important to emphasize that R19 and F20 are model-independent measures. We are using these additional priors to break the statistical degeneracy which characterizes our analysis shown in the left panel of Fig. 4, especially in the H_0 parameter, where we use a very loose and flat prior: $H_0 \in [10, 90]$. The R19 and F20 measures acts to keep our constraints for H_0 close to the observed values and, additionally, to improve the constraints on the other parameters. In fact, the BH growth parameters have significant positive correlations with H_0 , mainly f_{Edd} when analyzed from SMBHs data only (see the left panel of Fig. 4).

The right panel of Fig. 4 shows the parametric space from the joint analysis SMBHs + R19 and SMBH + F20. For the combination SMBH + R19, we find: $\log(M_i/M_\odot) > 4.5$ (at 95% CL), $H_0 = 74^{+1.5}_{-1.4} \text{ km s}^{-1}\text{Mpc}^{-1}$ and $f_{\text{Edd}} = 0.777^{+0.035}_{-0.026}$ at 68% CL. In the joint case SMBH + F20, we find: $\log(M_i/M_\odot) > 4.5$ (at 95% CL), $H_0 = 69.7^{+2.0}_{-2.1} \text{ km s}^{-1}\text{Mpc}^{-1}$ and $f_{\text{Edd}} = 0.730^{+0.040}_{-0.028}$ at 68% CL. We summarize our results for SMBH + R19 and SMBH + F20 as follows:

- The addition of R19 and F20 data improves the constraints on M_i by ~ 0.3 dex. Our analysis show that the presence of quasars at $z \gtrsim 6.5$ strongly favors the formation of BH seeds with mass $M_\bullet > 10^4 M_\odot$.
- Regarding the parameters of the BH growth model, we note an improvement by 10.86% and 9.58% on f_{Edd} from the addition of R19 and F20 data, respectively.

This analysis confirms that Hubble parameter data can be fundamental to improve the constraints on the parameters of the BH growth model.

As a complementary information to the best fit values, Table 2 reports the correlation matrix for the parameters resulting from the analysis SMBH + R19 (the corresponding table for SMBH + F20 is

Table 2. Correlation matrix for the parameters of the BH mass growth model (SMBH + R19 data).

	$\log(M_i/M_\odot)$	h	f_{Edd}
$\log(M_i/M_\odot)$	1.00	-0.01	-0.89
h	-0.01	1.00	0.43
f_{Edd}	-0.89	0.43	1.00

very similar). We emphasize that there is a strong anti-correlation between the parameters M_i and f_{Edd} , as expected from their physical interpretation. Also, we note a positive-correlation between f_{Edd} and H_0 . This warrants a careful choice of the combination of these parameters whenever running numerical simulations.

5 FINAL REMARKS

We have investigated the effect that the value of the Hubble parameter H_0 has on models for the cosmic growth of BH seeds, by using an MCMC technique to fit mass measurements for $z \geq 6.5$ quasars. First, we noted that the predicted mass for a BH at $z = 6$ changes by $> 300\%$ if H_0 is changed from 65 to 74 $\text{km s}^{-1}\text{Mpc}^{-1}$. Assuming that seed formation occurs at $z \sim 25$, we find a strong preference for heavy seeds with $\log(M_i/M_\odot) > 4$ in all our models. With the specific priors on quasars used, light seed formation scenarios are rejected in our model at $\sim 3\sigma$. Our analysis is improved by considering gaussian priors on the value of H_0 , specifically $H_0 = 74.03 \pm 1.42 \text{ km s}^{-1}\text{Mpc}^{-1}$ (Riess et al. 2019, or R19) and $69.6 \pm 2.0 \text{ km s}^{-1}\text{Mpc}^{-1}$ (Freedman et al. 2019, or F20). When considering the joint analysis SMBH + R19 and SMBH + F20, the priors on the value of the Hubble parameter significantly improve the constraints on f_{Edd} . We find that the Eddington ratio can be estimated with an accuracy of $\sim 3.9\%$ and $\sim 4.6\%$ from SMBH + R19 and SMBH + F20, respectively. Without targeted priors on H_0 , we can constrain f_{Edd} only with an accuracy of $\sim 33\%$. Of course, additional efforts are needed to better constrain the parameters of BH growth model: numerical and semi-analytical simulations, as well as additional data sets for high- z quasars, will provide better estimates. On the other hand, we showed that measurements of the Hubble parameter are fundamental to improve the constraints on these parameters.

We recognize that there is a fundamental difference between the BH growth parameters and the value of the Hubble parameter. While the former parameters depend on the local accretion conditions and, in general, each BH is characterized by a different, possibly time-variable, combination of (M_i, f_{Edd}) , the latter is a constant value. Hence, constraining the Hubble parameter by improving our knowledge on (M_i, f_{Edd}) seems realistic only with a very large statistical sample of high- z quasars. Despite this, we showed that there is a strong correlation between the Hubble parameter and the BH growth parameters: their combined analysis can thus bring a new perspective in the study of the farthest quasars.

An additional contribution to cosmology from the study of quasars could come from low- z observations. The Universe is currently undergoing an accelerated expansion and a complete explanation of this observation is still lacking. The concordance model thus far calls for an exotic component of dark energy, at low- z , to accelerate the cosmological expansion. Concurrently, the vast majority of AGNs (or accreting SMBHs at the center of galaxies) is currently detected at low redshift. Therefore, it could be fruitful to study how a background expansion of the Universe in the presence

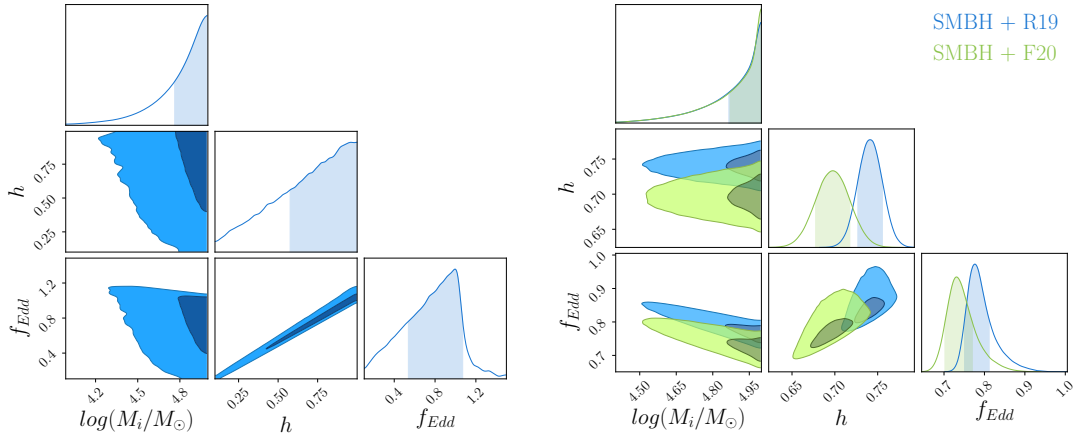


Figure 4. Left panel: Two-dimensional marginalized distributions of the free parameters M_i , H_0 , f_{Edd} at 1σ (darker area) and 2σ CL (lighter area) from SMBHs data only. Here, h is the reduced Hubble parameter, $H_0/100$ in units of $\text{km s}^{-1}\text{Mpc}^{-1}$. Right panel: Same as in left panel, but from the joint analysis SMBH + gaussian priors on H_0 .

of well-motivated dark energy models can also influence SMBH mass estimates at low- z , and vice versa. As the lookback time is very sensitive to the density parameter of dark energy at low z , a modified background expansion could significantly change the mass growth of BHs in the nearby Universe. We defer this investigation to a future communication.

ACKNOWLEDGEMENTS

The authors thank the referee for her/his very constructive comments and suggestions. RCN would like to thank the Brazilian Agency FAPESP for financial support under Project No. 2018/18036-5. FP acknowledges support from a Clay Fellowship administered by the Smithsonian Astrophysical Observatory and from the Black Hole Initiative at Harvard University, which is funded by grants from the John Templeton Foundation and the Gordon and Betty Moore Foundation.

REFERENCES

- Amaro-Seoane P., et al., 2017, arXiv e-prints, p. [arXiv:1702.00786](#)
 Bañados E., Decarli R., Walter F., Venemans B. P., Farina E. P., Fan X., 2015, *ApJ*, **805**, L8
 Bañados E., et al., 2016, *ApJS*, **227**, 11
 Bañados E., et al., 2018a, *Nature*, **553**, 473
 Bañados E., et al., 2018b, *Nature*, **553**, 473
 Bardeen J. M., 1970, *Nature*, **226**, 64
 Barkana R., Loeb A., 2001, *Phys. Rep.*, **349**, 125
 Barret D., Decourchelle A., Fabian A., Guainazzi M., Nandra K., Smith R., den Herder J.-W., 2020, *Astronomische Nachrichten*, **341**, 224
 Begelman M. C., Volonteri M., 2017, *MNRAS*, **464**, 1102
 Bromm V., Loeb A., 2003, *ApJ*, **596**, 34
 Carnall A. C., et al., 2015, *MNRAS*, **451**, L16
 Davies M. B., Miller M. C., Bellovary J. M., 2011, *ApJ*, **740**, L42
 Devecchi B., Volonteri M., 2009, *ApJ*, **694**, 302
 Devecchi B., Volonteri M., Rossi E. M., Colpi M., Portegies Zwart S., 2012, *MNRAS*, **421**, 1465
 Fan X., et al., 2006, *AJ*, **131**, 1203
 Foreman-Mackey D., Hogg D. W., Lang D., Goodman J., 2013, *PASP*, **125**, 306
 Freedman W. L., et al., 2019, *ApJ*, **882**, 34
 Gallerani S., Fan X., Maiolino R., Pacucci F., 2017, *Publ. Astron. Soc. Australia*, **34**, e022
 Gelman A., Rubin D. B., 1992, *Statistical Science*, **7**, 457
 Haiman Z., Loeb A., 2001, *The Astrophysical Journal*, **552**, 459
 Hirano S., Hosokawa T., Yoshida N., Umeda H., Omukai K., Chiaki G., Yorke H. W., 2014, *The Astrophysical Journal*, **781**, 60
 Inayoshi K., Visbal E., Haiman Z., 2019, arXiv e-prints, p. [arXiv:1911.05791](#)
 Jiang L., et al., 2009, *The Astronomical Journal*, **138**, 305
 Katz H., Sijacki D., Haehnelt M. G., 2015, *MNRAS*, **451**, 2352
 Kumar S., Nunes R. C., Yadav S. K., 2019, *European Physical Journal C*, **79**, 576
 Latif M., Schleicher D., 2019, Formation of the First Black Holes, [doi:10.1142/10652](#).
 Lodato G., Natarajan P., 2006, *MNRAS*, **371**, 1813
 Lupi A., Colpi M., Devecchi B., Galanti G., Volonteri M., 2014, *MNRAS*, **442**, 3616
 Madau P., Haardt F., Dotti M., 2014, *ApJ*, **784**, L38
 Matsuoka Y., et al., 2016, *ApJ*, **828**, 26
 Matsuoka Y., et al., 2019, *The Astrophysical Journal*, **872**, L2
 Mortlock D. J., et al., 2011, *Nature*, **474**, 616
 Mushotzky R., et al., 2019, in BAAS. p. 107 ([arXiv:1903.04083](#))
 Narayan R., McClintock J. E., 2013, arXiv e-prints, p. [arXiv:1312.6698](#)
 Novikov I. D., Thorne K. S., 1973, in Black Holes (Les Astres Occlus). pp 343–450
 Pacucci F., Loeb A., 2020, arXiv e-prints, p. [arXiv:2004.07246](#)
 Pacucci F., Volonteri M., Ferrara A., 2015, *MNRAS*, **452**, 1922
 Pacucci F., Natarajan P., Ferrara A., 2017a, *ApJ*, **835**, L36
 Pacucci F., Natarajan P., Volonteri M., Cappelluti N., Urry C. M., 2017b, *The Astrophysical Journal*, **850**, L42
 Pelupessy F. I., Di Matteo T., Ciardi B., 2007, *ApJ*, **665**, 107
 Planck Collaboration et al., 2018, arXiv e-prints, p. [arXiv:1807.06209](#)
 Reed S. L., et al., 2015, *MNRAS*, **454**, 3952
 Reed S. L., et al., 2017, *MNRAS*, **468**, 4702
 Regan J. A., Downes T. P., Volonteri M., Beckmann R., Lupi A., Trebitsch M., Dubois Y., 2019, *MNRAS*, **486**, 3892
 Ricarte A., Natarajan P., 2018, *MNRAS*, **474**, 1995
 Riess A. G., Casertano S., Yuan W., Macri L. M., Scolnic D., 2019, *The Astrophysical Journal*, **876**, 85
 Salpeter E. E., 1955, *ApJ*, **121**, 161
 Shakura N. I., Sunyaev R. A., 1976, *MNRAS*, **175**, 613
 Shankar F., Weinberg D. H., Miralda-Escudé J., 2009, *ApJ*, **690**, 20
 Shapiro S. L., 2005, *The Astrophysical Journal*, **620**, 59
 Shen Y., et al., 2007, *AJ*, **133**, 2222
 Tanaka T., Haiman Z., 2009a, *ApJ*, **696**, 1798

- Tanaka T., Haiman Z., 2009b, [ApJ](#), **696**, 1798
- The Lynx Team 2018, arXiv e-prints, p. [arXiv:1809.09642](#)
- Venemans B. P., McMahon R. G., Warren S. J., Gonzalez-Solares E. A., Hewett P. C., Mortlock D. J., Dye S., Sharp R. G., 2007, [MNRAS](#), **376**, L76
- Venemans B. P., et al., 2013, [ApJ](#), **779**, 24
- Venemans B. P., et al., 2015, [ApJ](#), **801**, L11
- Venemans B. P., Walter F., Zschaechner L., Decarli R., De Rosa G., Findlay J. R., McMahon R. G., Sutherland W. J., 2016, [ApJ](#), **816**, 37
- Verde L., Treu T., Riess A. G., 2019, [Nature Astronomy](#), **3**, 891
- Volonteri M., Rees M. J., 2005, [The Astrophysical Journal](#), **633**, 624
- Volonteri M., Silk J., Dubus G., 2015, [ApJ](#), **804**, 148
- Wang F., et al., 2018, [The Astrophysical Journal](#), **869**, L9
- Willott C. J., et al., 2010, [The Astronomical Journal](#), **140**, 546
- Wong K. C., et al., 2019, arXiv e-prints, p. [arXiv:1907.04869](#)
- Wu X.-B., et al., 2015, [Nature](#), **518**, 512